

Discovery of controllable high Chern number quantum anomalous Hall state in tetragonal lattice FeSIn

Xiao-Lang Ren(任小浪) and Chang-Wen Zhang(张昌文)

Citation: Chin. Phys. B, 2024, 33 (**6**): 067102. DOI: 10.1088/1674-1056/ad2bf1
Journal homepage: http://cpb.iphy.ac.cn; http://iopscience.iop.org/cpb

What follows is a list of articles you may be interested in

Magnetism, heat capacity, magnetocaloric effect, and magneto-transport properties of heavy fermion antiferromagnet CeGaSi

Li-Bo Zhang(张黎博), Qing-Xin Dong(董庆新), Jian-Li Bai(白建利), Qiao-Yu Liu(刘乔宇), Jing-Wen Cheng(程靖雯), Cun-Dong Li(李存东), Pin-Yu Liu(刘品宇), Ying-Rui Sun(孙英睿), Yu Huang(黄宇), Zhi-An Ren(任治安), and Gen-Fu Chen(陈根富)
Chin. Phys. B, 2024, 33 (**6**): 067101. DOI: 10.1088/1674-1056/ad3060

Two-dimensional transition metal halide PdX_2(X= F, Cl, Br, I): A promising candidate of bipolar magnetic semiconductors

Miao-Miao Chen(陈苗苗), Sheng-Shi Li(李胜世), Wei-Xiao Ji(纪维霄), and Chang-Wen Zhang(张昌文)
Chin. Phys. B, 2023, 32 (**12**): 127103. DOI: 10.1088/1674-1056/ad04c3

Coherent interaction and action-counteraction theory in small polaron systems, and ground state properties

Zhi-Hua Luo(罗质华) and Chao-Fan Yu(余超凡)
Chin. Phys. B, 2022, 31 (**11**): 117104. DOI: 10.1088/1674-1056/ac67c1

Properties of ground state and anomalous quantum fluctuations in one-dimensional polaron–soliton systems—the effects of electron-two-phonon interaction and non-adiabatic quantum correlations

Luo Zhi-Hua(罗质华), Cao Xi-Jin(曹锡金), and Yu Chao-Fan(余超凡)
Chin. Phys. B, 2011, 20 (**6**): 067103. DOI: 10.1088/1674-1056/20/6/067103

Discovery of controllable high Chern number quantum anomalous Hall state in tetragonal lattice FeSIn

Xiao-Lang Ren(任小浪) and Chang-Wen Zhang(张昌文)†

School of Physics and Technology, Institute of Spintronics, University of Jinan, Jinan 250022, *China*

(Received 12 December 2023; revised manuscript received 7 February 2024; accepted manuscript online 22 February 2024)

Quantum anomalous Hall (QAH) insulators have excellent properties driven by fancy topological physics, but their practical application is greatly hindered by the observed temperature of liquid nitrogen, and the QAH insulator with high Chern number is conducive to spintronic devices with lower energy consumption. Here, we find that monolayer FeSIn is a good candidate for realizing the QAH phase; it exhibits a high magnetic transition temperature of 221 K and tunable $C = \pm 2$ with respect to magnetization orientation in the y–z plane. After the application of biaxial strain, the magnetic axis shifts from the x–y plane to the z direction, and the effect of the high C and ferromagnetic ground state on the stress is robust. Also, the effect of correlation U on C has been examined. These properties are rooted in the large size of the Fe atom that contributes to ferromagnetic kinetic exchange with neighboring Fe atoms. These findings demonstrate monolayer FeSIn to be a major template for probing novel QAH devices at higher temperatures.

Keywords: high Chern number, Weyl semimetals, quantum anomalous Hall insulator, magnetic transition temperature

PACS: 71.38.Mx, 75.50.Pp, 73.20.At **DOI:** 10.1088/1674-1056/ad2bf1

1. Introduction

The quantum anomalous Hall (QAH) effect has garnered widespread attention in the study of magnetic topological materials.[1–5] On account of its dissipationless chiral edge states, the QAH effect can be utilized to manufacture next-generation low-power-consumption spin electronic devices, and offers a predominant platform for investigating peculiar quantum physics, such as topological magneto-electric effects and topological superconductivity.[6–9] Indeed, the QAH effect as a far-reaching research field that is currently developing rapidly, and a multitude of candidates have been theoretically predicted to host the QAH effect.[10–21] Although the QAH effect has been successfully implemented in Cr-doped $(Bi, Sb)_2Te_3$,[22] the observed temperature of liquid nitrogen seriously limits its practical application. The realization of the QAH effect must satisfy ferromagnetic exchange of 3d elements under spin–orbit coupling (SOC) of heavy elements, so QAH materials are rare. Recently, the observed temperature has been increased to 1.4 K in intrinsic $MnBi_2Te_4$ thin film,[23] so intrinsic QAH insulators have been searched for to increase the observed temperature. A great deal of effort has been made to explore the intrinsic QAH effect, such as in two-dimensional (2D) FeI_2,[24] Li-decorated FeX (X = S, Se, Te) [25] and twisted bilayer graphene.[26] Despite these latest findings, it remains an urgent challenge to find more intrinsic QAH materials with a large band gap that can dependably operate at room or higher temperatures with robust structural and property stability.

In addition to the question of observed temperature, finding QAH states with a high Chern number (C) remains a profound challenge. QAH states with a high C can provide more dissipationless chiral edge channels, so the material can be used to make electronic devices with extremely low power consumption. At this juncture, although topological materials with high C, such as monolayer TiTe,[27] monolayer XTiY,[28] and monolayer $NiBiO_3$,[29] have been proposed, the search for topological insulators with high C is still a crucial topic. Because of their numerous excellent properties, 2D materials have aroused widespread attention.[30–32]

In this paper, we scientifically investigate the stability, magnetic, electronic and topological properties of monolayer FeSIn crystallized in the $P4/nmm$ space group by performing the first-principles simulations. It is predicted to be structurally stable by phonon spectra, elastic constants, formation energy and molecular dynamics simulations. We show that monolayer FeSIn is an x–y easy-plane ferromagnetic (FM) Weyl semimetal with a high Berezinskii–Kosterlitz–Thouless (BKT) magnetic transition temperature (221 K). Four Dirac points appear in the first Brillouin zone (BZ) due to C_4 and inversion symmetries. When SOC is taken into account, the sizeable band gap is opened at the Dirac points to host the QAH state. Moreover, a topological phase transition from $C = 2$ to $C = -2$ can be realized by turning the magnetization direction. We further find that magnetocrystalline anisotropy energy (MAE) can be effectively regulated by the compressive strain, so that the magnetization orientation is changed and a QAH state with high C can be achieved. Meanwhile, with increase in U, the band gap will gradually increase. When

†Corresponding author. E-mail: ss_zhangchw@ujn.edu.cn

© 2024 Chinese Physical Society and IOP Publishing Ltd

U is greater than 3.7 eV, the direct band gap is transformed into an indirect band gap, and the band gap will gradually decreases. Interestingly, the magnetic topological state is robust to changes in the value of U.

2. Methods

The electronic properties of monolayer FeSIn are researched by employing first-principles density-functional theory (DFT).[33–35] Because of the correlation effects of 3d electrons in Fe atoms, we employed the generalized gradient approximation (GGA) $+U$ approach within the Dudarev scheme.[36] Here, we study the properties of monolayer FeSIn at $U_{\text{eff}} = 1$–4 eV. Meanwhile, the Hubbard correction $U_{\text{eff}} = 2.5$ eV[37–39] is mainly employed to discuss monolayer FeSIn. A plane-wave basis with a kinetic energy cutoff of 500 eV is employed. The first BZ is sampled by Γ-centered Monkhorst–Pack grids of $21 \times 21 \times 1$.[40] The vacuum layer is set to 28 Å to avoid coupling between the periodic layers. All the atoms are allowed to relax until the atomic force on each atom is smaller than 0.001 eV·Å^{-1}. The convergence criterion for the total energies is set to be 10^{-7} eV. The phonon spectra is calculated using density-functional perturbation theory as implemented in the PHONOPY code.[41] Surface states are calculated with WANNIER90[42] and WANNIERTOOLS packages.[43]

2.1. Structure and stabilities

Monolayer FeSIn is a layered tetragonal crystal with space group $P4/nmm$ (No. 129) as shown in Fig. 1(a). The Fe atoms per unit cell lie on the identical plane, and the nonmagnetic S and In atoms are distributed on both sides of the center plane in a staggered order [see Fig. 1(a)]. The calculated lattice constant for monolayer FeSIn is 3.78 Å, and the nearest Fe–Fe distance and Fe–S bond length for monolayer FeSIn are 2.67 Å and 2.42 Å, respectively. The formation energy can be obtained from the equation

$$E_{\text{form}} = (2E_{\text{Fe}} + 2E_{\text{S}} + 2E_{\text{In}} - 2E_{\text{FeSIn}})/6, \quad (1)$$

where E_{Fe}, E_{In} and E_{S} are the energy of single Fe, In and S atoms in its most stable bulk structure and E_{FeSIn} is the total energy per unit cell of monolayer FeSIn; the calculated formation energy is 0.627 eV/atom, which proves that monolayer FeSIn is easier to form than pure S, In and Fe structures. The dynamical stability of monolayer FeSIn is investigated by calculating the phonon spectra, and MD simulation is performed to demonstrate the thermal stability. As shown in Fig. 1(d), the dynamical stability of monolayer FeSIn is manifested by the phonon spectra with no negative frequency in the whole BZ. The results of the MD simulation indicate that monolayer FeSIn remains intact at 300 K after 8 fs [see Fig. 1(c)]. Finally, to prove the mechanical stability of the tetragonal structure FeSIn, the elastic constants C_{11}, C_{22}, C_{12} and C_{66} of monolayer FeSIn are calculated as 77.8 N·m^{-1}, 77.8 N·m^{-1}, 50.35 N·m^{-1} and 17.5 N·m^{-1}, respectively, which meet the Born–Huang criteria of C_{11}, C_{22}, $C_{66} > 0$ and $C_{11} + C_{22} - 2C_{12} > 0$. The mechanical stability of monolayer FeSIn is manifested.

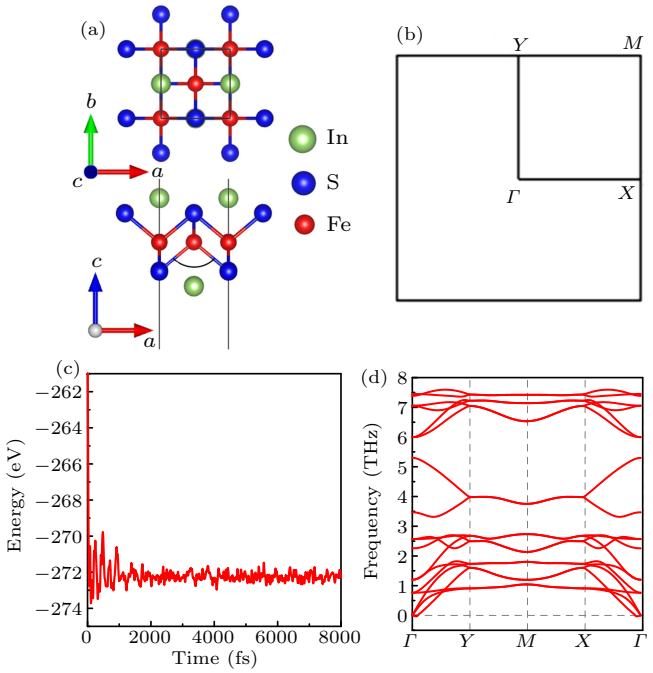


Fig. 1. (a) Top and side views of monolayer FeSIn. (b) The first Brillouin zone of monolayer FeSIn. (c), (d) The phonon dispersion and time evolution of free energy during the molecular dynamics calculations for monolayer FeSIn.

3. Results and discussion

To reveal the magnetic ground state of monolayer FeSIn, we consider four kinds of magnetic structures, i.e., (i) ferromagnetic (FM), (ii) antiferromagnetic 1 (AFM1), (iii) AFM2 and (iv) AFM3 [see Fig. S1]. The total energies are listed in Fig. 5(a), which indicates that monolayer FeSIn prefers the FM ground state. The nearest-neighbor transitional metal Fe atoms are linked by S atoms, implying that the magnetic ground state is determined by the super-exchange mechanism. The bond angle of Fe–S–Fe in monolayer FeSIn is 102.6°, closing to 90°, according to the Goodenough–Kanamori rules; this is conducive to ferromagnetic interaction. On the basis of the Mermin–Wagner theorem,[44] long-range magnetic order is generally forbidden in isotropic one-dimensional or 2D systems at nonzero temperatures. Hence, magnetic anisotropy is crucial for a 2D material to remain in a long-range FM ground state. The magnetic moment of monolayer FeSIn is 3 μ_{B}. The MAE can be expressed as MAE $= E_{100} - E_{001}$, and the calculated MAE is -0.377 meV, which illustrates magnetization direction of monolayer FeSIn lies in the x–y plane. According to BKT, magnetic transition temperature of monolayer FeSIn

is 221 K (see supporting material for details). For monolayer FeSIn, total energy as a function of the angle (θ) between the magnetization direction within the y–z plane and the x-axis is plotted in Fig. 2(c) and can be obtained by the following equation:

$$E(\theta) = E_e + K_1 \cos^2\theta + K_2 \cos^4\theta, \tag{2}$$

where E_e is the total energy of monolayer FeSIn with the magnetization direction along the easy axis and K_1 and K_2 are quadratic and quartic constants, respectively. For monolayer FeSIn, K_1 and K_2 are 0.39 and 2.55 meV, and we can see the distinct magnetic anisotropy from Fig. 2(c). The evident magnetic anisotropy is beneficial to stabilize the FM ground states against thermal fluctuation in monolayer FeSIn.

We now study the electronic band structure of monolayer FeSIn. Figures 3(a) and 3(b) show the calculated band structure of monolayer FeSIn with and without consideration of SOC. The linear crossings are formed by two spin-down bands, which are observed at E_F for monolayer FeSIn. The conduction and valence bands are connected by these. Four spin-polarized Dirac cones emerge in the first BZ due to the C_4 and inversion symmetries [see Fig. 1(b)]. Thus, monolayer FeSIn can be called a Weyl semimetal with 100% spin polarization in the absence of SOC. The Dirac cones of monolayer FeSIn are primarily contributed to by the spin-down d_{xy} and $d_{x^2-y^2}$ orbits of the Fe atom [see Figs. 2(a) and 2(b)].

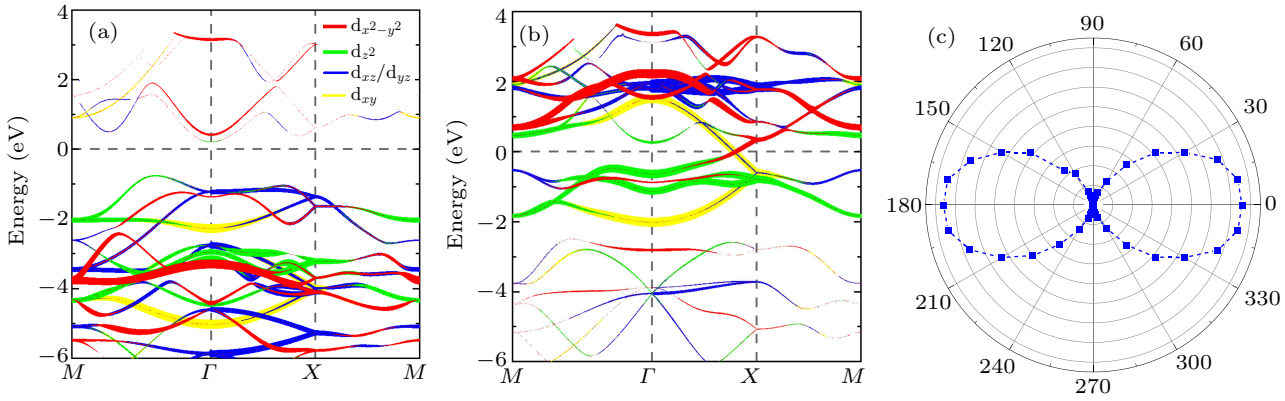


Fig. 2. (a), (b) The d-orbital resolved spin-polarized band structures in spin-up and spin-down channels of monolayer FeSIn, respectively. (c) Total energy per unit cell of monolayer FeSIn as a function of the angle (θ) in the y–z plane.

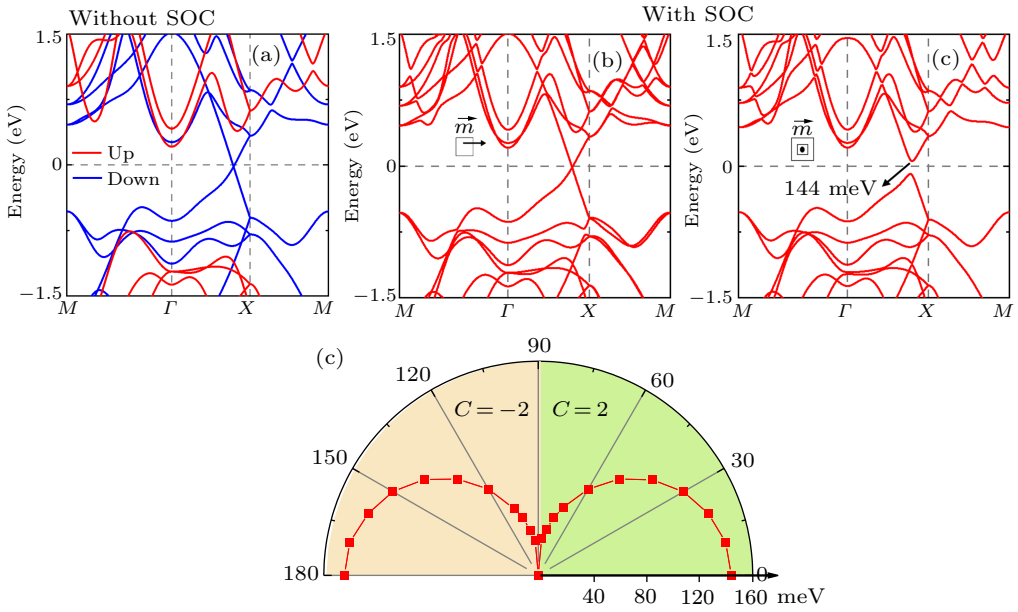


Fig. 3. Spin polarized band structure of monolayer FeSIn without SOC (a) and with SOC (b) when the magnetization direction lies in the y and z directions. Band gaps of monolayer FeSIn with the magnetization direction varying from $\theta = 0°$ to $\theta = 180°$ in the y–z plane. The light green and light brown areas show monolayer FeSIn with Chern numbers C of 2 and −2, respectively.

When SOC is turned on, the magnetization direction lies in the x–y plane and the linear crossings remain at E_F, which means that monolayer FeSIn can be used to fabricate high-performance spin field-effect transistors or magnetic tunnel junctions with 100% tunneling magnetoresistance in spintronics.[45] Importantly, when the magnetization direction is shifted to the z direction, a sizeable band gap of 144 meV is opened [see Fig. 3(b)]; this band gap value is much larger than that of many materials that have been reported, such as monolayer $PdSbO_3$ (23.4 meV),[46] monolayer

OsI_3 (118.3 meV)[47] and monolayer YN_2 (29.7 meV).[48] To probe the electronic band characteristics along different magnetization directions, we consider different magnetization orientations. When the magnetization direction is rotated from the $+z$-axis to the y-axis, as the z-component of the magnetization orientation diminishes the band gap gradually decreases. When magnetization lies in the y direction, the band gap closes and the linear crossings appear again at E_F, as shown in Figs. S2(a)–S2(f).

With SOC turned on, we systematically study the topological properties of monolayer FeSIn. In order to demonstrate the topological properties of monolayer FeSIn, the chiral edge states of monolayers FeSIn are calculated. The conduction and valence bands are connected by two dissipationless chiral edge channels, as shown in Fig. 4(a), which signify that the large band gap of 144 meV is nontrivial. Importantly, the nontrivial band gap is conducive to observing the QAH effect with high C at higher temperature. To indicate the topological properties of monolayer FeSIn, C is obtained by the following equation:

$$C = \frac{1}{2\pi}\int_{BZ} d^2k\Omega_n(k), \tag{3}$$

where $\Omega_z(k)$ is the Berry curvature of the 2D system. According to the above equation, C of an FeSIn monolayer in the whole BZ is 2. The anomalous Hall conductance is calculated and can be obtained from the equation

$$\sigma = \frac{e^2}{h}\frac{1}{2\pi}\int_{BZ} d^2k\Omega_n(k). \tag{4}$$

The non-zero anomalous Hall conductance proves that monolayer FeSIn is an excellent QAH template, as shown in Fig. 4(c). Meanwhile, Berry curvature can help us further understand the high $C = 2$; Berry curvature is calculated with following equation:

$$\Omega(k) = -\sum_{n<E_F}\sum_{m\neq n} 2\,\mathrm{Im}\frac{\langle\Psi_{n\boldsymbol{k}}|v_x|\Psi_{m\boldsymbol{k}}\rangle\langle\Psi_{m\boldsymbol{k}}|v_y|\Psi_{n\boldsymbol{k}}\rangle}{(\varepsilon_{m\boldsymbol{k}}-\varepsilon_{n\boldsymbol{k}})^2}, \tag{5}$$

where m and n are band indices and $\psi_{m/n\boldsymbol{k}}$, $\varepsilon_{m/n\boldsymbol{k}}$ and $v_{x/y}$ express the Bloch wave functions, corresponding eigenenergies of band m/n and the velocity operators, respectively. Each of the four opening band gaps gives a topological charge of 0.5, resulting in $C = 2$ for monolayer FeSIn in Fig. 4(e), which further suggests that the monolayer is a topological insulator with high C. Interestingly, when the magnetization direction is along the y direction, monolayer FeSIn is a Weyl semimetal. However, the magnetization direction is rotated from the $+z$ direction to the $-z$ direction, and a high-C topological phase transition occurs from $C = 2$ to $C = -2$, as shown in Fig. 3(c), which means that electrons can be transported in the opposite direction. This non-zero anomalous Hall conductance and Berry curvature further confirm this finding [see Figs. 3(b), 3(d) and 3(f)]. In addition, as illustrated in Figs. S4(a)–S4(d) a similar material (FeTeGa) also exhibits the QAH effect with high C, reflecting that these excellent properties may occur in more tetragonal lattice compounds.

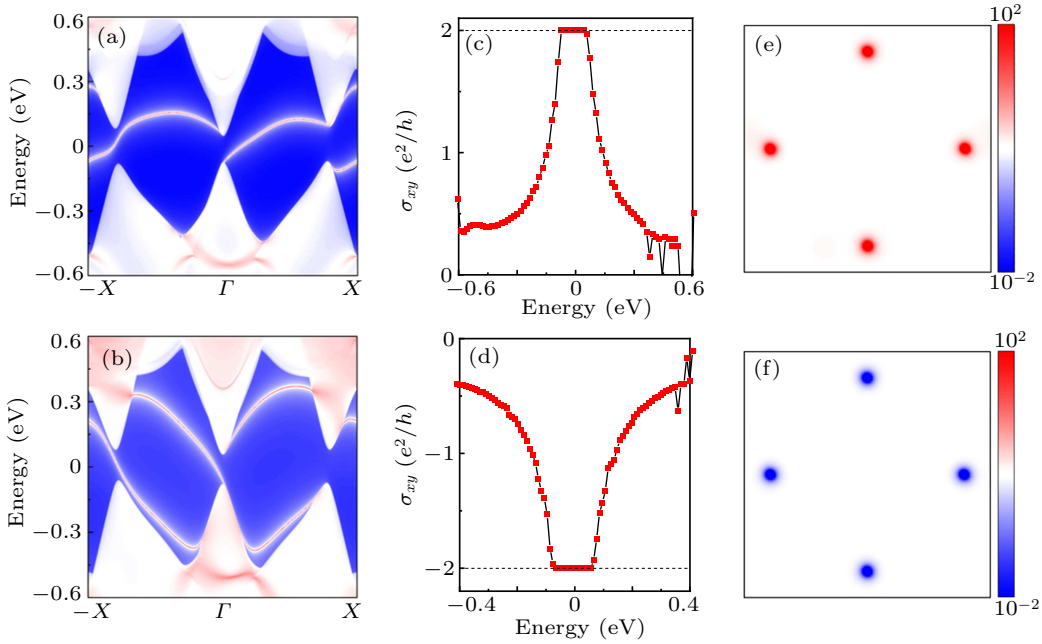


Fig. 4. Edge states, and corresponding anomalous Hall conductance and distribution of the Berry curvature for monolayer FeSIn with magnetization direction in the z ((a), (c), (e)) and $-z$ ((b), (d), (f)) directions.

Because of the flexibility of 2D materials, these various material properties can be effectively turned by applying strain. Here, the effect of strain on monolayer FeSIn is checked by applying biaxial strain from -3% to $+3\%$. As displayed in Fig. 5(d), from compressive strain to tensile the MAE decreases monotonically. Importantly, when compres-

sive strain is applied, magnetization direction shifts from the x–y plane to the z direction, which is conducive to the generation of a topological state with high C. Meanwhile, the QAH state and FM ground state of monolayer FeSIn are robust to biaxial strain, as shown in Figs. 5(b) and 5(f). In order to explore the influence of the U value on the ground state and MAE, different U values are considered. The ground state and MAE are robust to the changed U values [see Figs. 5(a) and 5(c)]. With increase in the U value the band gap will gradually increase, which is beneficial for observing the QAH effect at room temperature. When the U value is greater than 3.7 eV, the direct band gap shifts to an indirect band gap and the band gap gradually decreases. Interestingly, the topological state with high C does not disappear with the change in U value, as displayed in Fig. 5(e).

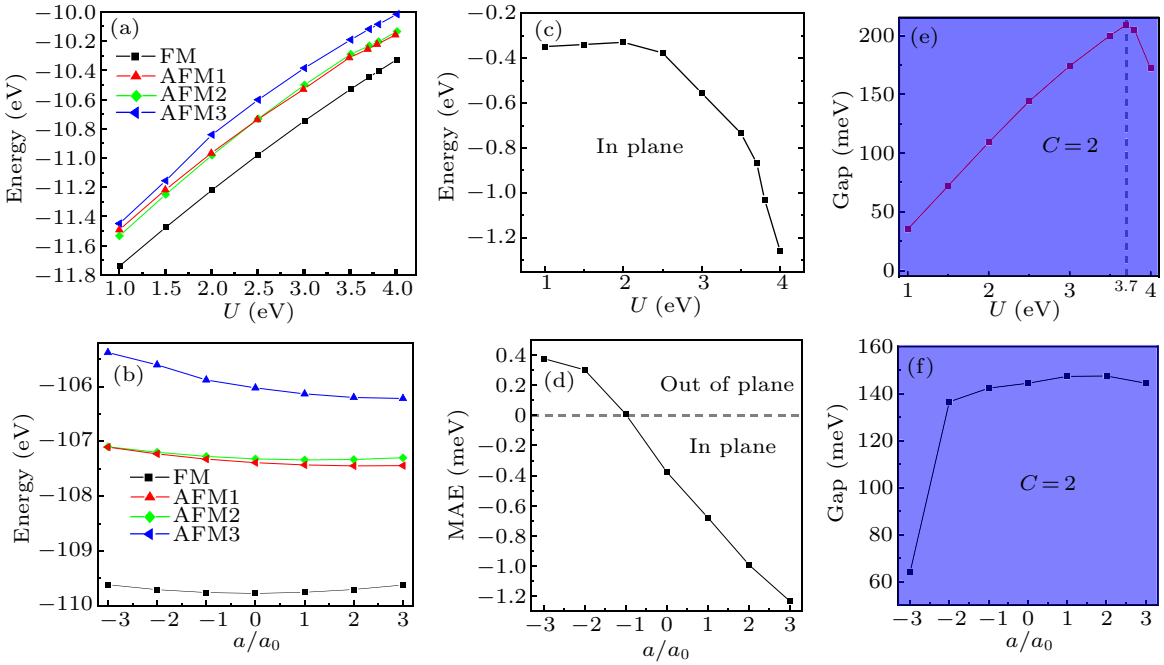


Fig. 5. (a) The FM and AFM energies of monolayer FeSIn as a function of the on-site Hubbard U, respectively. (b) The energy differences between FM and different AFM states of monolayer FeSIn as a function of applied biaxial strain. (c), (d) The MAE of monolayer FeSIn as a function of the on-site Hubbard U and biaxial strain. (e), (f) The band gap and Chern number of monolayer FeSIn as a function of the on-site Hubbard U and strain when magnetization is along the z-direction.

4. Conclusion

We have systematically probed the electronic and topological properties of stable monolayer FeSIn based on first-principles simulations; the dynamical, mechanical and thermal stabilities are verified by phonon spectrum calculations, calculated elastic constants and MD simulations. When SOC is turned on, the system is changed to an FM QAH insulator of high C with a sizeable band gap. By turning the magnetization direction, topological phase transition from $C = 2$ to $C = -2$ arises in monolayer FeSIn. Importantly, when compressive strain is applied, the magnetic axis shifts from the x–y plane to the z direction, which facilitates the generation of a spontaneous QAH state with high C. Meanwhile, the magnetic ground state and MAE are robust to the U value, and the band gap gradually increases with increase in the U value, which is conducive to the experimental observation of a QAH state. Moreover, QAH states with high C are robust to biaxial strain and U-value. We also found that the similar excellent properties are likely to occur in monolayer FeTeGa. Our findings provide insights for lower-energy-consumption spintronic devices and observation of higher-temperature QAH states.

Acknowledgements

Project supported by the National Natural Science Foundation of China (Grant No. 52173283), the Taishan Scholar Program of Shandong Province, China (Grant No. ts20190939), and the Independent Cultivation Program of Innovation Team of Jinan City (Grant No. 2021GXRC043).

References

[1] Chang C Z, Liu C X and MacDonald A H 2023 *Rev. Mod. Phys.* **95** 011002
[2] Weng H, Yu R, Hu X, Dai X and Fang Z 2015 *Adv. Phys.* **64** 227
[3] Sun H, Li S S, Ji W X and Zhang C W 2022 *Phys. Rev. B* **105** 195112
[4] Liu C X, Zhang S C and Qi X L 2016 *Annu. Rev. Condens. Matter Phys.* **7** 301
[5] Haldane F D M 1988 *Phys. Rev. Lett.* **61** 2015
[6] He K, Wang Y and Xue Q K 2018 *Annu. Rev. Condens. Matter Phys.* **9** 329
[7] Qi X L, Hughes T L and Zhang S C 2010 *Phys. Rev. B* **82** 184516
[8] Qi X L, Hughes T L and Zhang S C 2008 *Phys. Rev. B* **78** 195424
[9] Xiao D, Jiang J, Shin J H, Wang W F, Zhao Y F, Liu C, Wu W, Chan M H W, Samarth N and Chang C Z 2018 *Phys. Rev. Lett.* **120** 056801

[10] Yu R, Zhang W, Zhang H J, Zhang S C, Dai X and Fang Z 2010 *Science* **329** 61
[11] Han Y T, Ji W X, Wang P J, Li P and Zhang C W 2023 *Nanoscale* **15** 6830
[12] Zhang H, Xu Y, Wang J, Chang K and Zhang S C 2014 *Phys. Rev. Lett.* **112** 216803
[13] Zhang M H, Zhang C W, Wang P J and Li S S 2018 *Nanoscale* **10** 20226
[14] Qiao Z, Ren W, Chen H, Bellaiche L, Zhang Z, MacDonald A H and Niu Q 2014 *Phys. Rev. Lett.* **112** 116404
[15] Niu C, Bihlmayer G, Zhang H, Wortmann D, Blügel S and Mokrousov Y 2015 *Phys. Rev. B* **91** 041303
[16] Xu G, Wang J, Felser C, Qi X L and Zhang S C 2015 *Nano Lett.* **15** 2019
[17] Wang Y P, Ji W X, Zhang C W, Li P, Zhang S F, Wang P J, Li S S and Yan S S 2017 *Appl. Phys. Lett.* **110** 213101
[18] Wang Z F, Liu Z, Yang J and Liu F 2018 *Phys. Rev. Lett.* **120** 156406
[19] Zhang S J, Zhang C W, Zhang S F, Ji W X, Li P, Wang P J, Li S S and Yan S S 2017 *Phys. Rev. B* **96** 205433
[20] Otrokov M M, Rusinov I P, M. Rey B, Hoffmann M, Vyazovskaya A Y, Eremeev A Y, Ernst A, Echenique P M, Arnau A and Chulkov E V 2019 *Phys. Rev. Lett.* **122** 107202
[21] Guo P J, Liu Z X and Liu Z Y 2023 *npj Comput. Mater.* **9** 70
[22] Chang C Z, Zhang J S, Feng X, Shen J, Zhang Z C, Guo M, Li K, Ou Y, Wei P, Wang L L, Ji Z Q, Feng Y, Ji S H, Chen X, Jia J F, Dai X, Fang Z, Zhang S C, He K, Wang Y Y, Lu L, Ma X C and Xue Q K 2013 *Science* **340** 167
[23] Deng Y, Yu Y, Shi M Z, Wang M Z, Chen X H and Zhang Y 2020 *Science* **367** 895
[24] Sun Q L, Ma Y D and Kioussis N 2020 *Mater. Horiz.* **7** 2071
[25] Li Y, Li, Li Y, Ye M, Zheng F W, Zhang Z T, Fu J H, Duan W H and Xu Y 2020 *Phys. Rev. Lett.* **125** 086401
[26] Serlin M, Tschirhart C L, Polshyn H, Zhang Y, Zhu J, Watanabe K, Taniguchi T, Balents L and Young A F 2020 *Science* **367** 900
[27] Xuan X Y, Zhang Z H, Chen C F and Guo W L 2022 *Nano Lett.* **22** 5379
[28] Jiang Y D, Wang H and Wang J 2023 *Phys. Rev. B* **108** 165122
[29] Wu X M, Li R H, Zou X R, Huang B B, Dai Y and Niu C W 2023 *Phys. Rev. B* **108** 115438
[30] Wu B. Song Y L, Ji W X, Wang P J, Zhang S F and Zhang C W 2023 *Phys. Rev. B* **107** 214419
[31] Zhang M H, Zhang C W, Wand P J and Li S S 2018 *Nanoscale* **10** 20226
[32] Li S S, Ji W X, Hu S J, Zhang C W and Yan S S 2017 *ACS Appl. Mater. Inter.* **9** 41443
[33] Kresse G and Furthmüller J 1996 *Phys. Rev. B* **54** 11169
[34] Kresse G and Furthmüller J 1996 *Comput. Mater. Sci.* **6** 15
[35] Kresse G and Joubert D 1999 *Phys. Rev. B* **59** 1758
[36] Dudarev S L, Botton G A, Savrasov S Y, Humphreys C J and Sutton A P 1998 *Phys. Rev. B* **57** 1505
[37] Guo S D, Mu W Q, Xiao X B and Liu B G 2021 *Phys. Chem. Chem. Phys.* **23** 25994
[38] Li J Y, Yao Q S, Wu L, Hu Z X, Gao B Y, Wan X G and Liu Q H 2022 *Nat. Commun.* **13** 919
[39] Sun Q L, Ma Y D and Kioussis N 2020 *Materials Horiz.* **7** 2071
[40] Krukau A V, Vydrov O A, Izmaylov A F and Scuseria G E 2006 *J. Chem. Phys.* **125** 224106
[41] Togo A and Tanaka I 2015 *Scr. Mater.* **108** 1
[42] Pizzi G, Vitale V, Arita R, Blugel S, Freimuth F, Geranton G, Gibertini M, Gresch D, Johnson C, Koretsune T, Ibanez-Azpiroz J, Lee H, Lihm J M, Marchand D, Marrazzo A, Mokrousov Y, Mustafa J I, Nohara Y, Nomura Y, Paulatto L, Ponce S, Ponweiser T, Qiao J F, Thole F, Tsirkin S S, Wierzbowska M, Marzari N, Vanderbilt D, Souza I, Mostofi A A and Yates J R 2020 *J. Phys.: Condens. Matter* **32** 165902
[43] Wu Q, Zhang S, Song H F, Troyer M and Soluyanov A A 2018 *Comput. Phys. Commun.* **224** 405
[44] Mermin N D and Wagner H 1966 *Phys. Rev. Lett.* **17** 1133
[45] Žutić I, Fabian J and Sarma S D 2004 *Rev. Mod. Phys.* **76** 323
[46] Li Z, Han Y L and Qiao Z H 2022 *Phys. Rev. Lett.* **129** 036801
[47] Fang X T, Zhou B Z, Wang X C and Mi W B 2022 *Mater. Today Phys.* **28** 100847
[48] Kong X R, Li L Y, Leenaerts O, Wang W Y, Liu X J and Peeters F M 2018 *Nanoscale* **10** 8153